HHS Public Access

Author manuscript

Technology (Singap World Sci). Author manuscript; available in PMC 2020 April 14.

Published in final edited form as:

Technology (Singap World Sci). 2019 ; 7(3-4): 98–107. doi:10.1142/S2339547819500067.

First-in-human evaluation of a hand-held automated venipuncture device for rapid venous blood draws

Josh M. Leipheimer[1], **Max L. Balter**[1], **Alvin I. Chen**[1], **Enrique J. Pantin**[2], **Alexander E. Davidovich**[3], **Kristen S. Labazzo**[1], **Martin L. Yarmush**[1]

[1]Department of Biomedical Engineering, Rutgers University, Piscataway, NJ 08854, USA

[2]Robert Wood Johnson University Hospital, 1 Robert Wood Johnson Place, New Brunswick, NJ 08901, USA

[3]Icahn School of Medicine, Mount Sinai Hospital, 1 Gustave L. Levy Place, New York, NY 10029-5674, USA

Abstract

Obtaining venous access for blood sampling or intravenous (IV) fluid delivery is an essential first step in patient care. However, success rates rely heavily on clinician experience and patient physiology. Difficulties in obtaining venous access result in missed sticks and injury to patients, and typically require alternative access pathways and additional personnel that lengthen procedure times, thereby creating unnecessary costs to healthcare facilities. Here, we present the first-in-human assessment of an automated robotic venipuncture device designed to safely perform blood draws on peripheral forearm veins. The device combines ultrasound imaging and miniaturized robotics to identify suitable vessels for cannulation and robotically guide an attached needle toward the lumen center. The device demonstrated results comparable to or exceeding that of clinical standards, with a success rate of 87% on all participants ($n = 31$), a 97% success rate on nondifficult venous access participants ($n = 25$), and an average procedure time of 93 ± 30 s ($n = 31$). In the future, this device can be extended to other areas of vascular access such as IV catheterization, central venous access, dialysis, and arterial line placement.

Keywords

Medical Device; Robotics; Image-Guidance; Ultrasound; Vascular Access; Computer Vision; Machine Learning

AUTHOR CONTRIBUTIONS

M.L.Y. was responsible for study oversight and was the principal investigator. J.M.L. designed and developed the device for the study. J.M.L. and K.S.L. were responsible for preparing the study and patient recruitment and interviewing; K.S.L. was responsible for obtaining IRB approval. E.J.P. and A.E.D. were the attending clinicians during the study. J.M.L., M.L.B., and A.I.C. were responsible for analyzing study results. J.M.L. prepared figures and wrote the manuscript, with editorial assistance from M.L.B. and A.I.C. All listed authors reviewed and commented on the final manuscript.

COMPETING INTERESTS

All authors declare that they have no competing funding, employment, or personal financial interests.

INNOVATION

Obtaining peripheral venous access in patients is one of the most essential and common first steps taken in any clinical intervention. Challenges associated with difficult venous access (DVA) have pushed for the development of technologies to improve the accuracy of cannula placement. Imaging technologies such as ultrasound and near infrared (NIR) are used to identify suitable vessels for cannulation; however, these devices do not assist with the actual insertion itself, but instead still require trained clinicians to perform the venipuncture. Here, we present a hand-held robotic venipuncture device that combines ultrasound imaging with miniaturized robotics to both identify vessels for insertion and accurately insert the cannula into the target vessel. In this paper, we present results of the first-in-human evaluation of an automated venipuncture device for performing routine blood draws from peripheral forearm vessels of participants. The flexible device design also allows it to be configured for other potential applications, including pediatrics, intravenous (IV) catheterization, central venous access, dialysis, and arterial line placement.

INTRODUCTION

Venipuncture, the process of obtaining venous access for blood sampling or IV therapy, is the most common clinical procedure performed worldwide, with over 1.4 billion procedures annually in the United States alone[1,2]. Traditionally, venipuncture is performed by trained clinicians and phlebotomists, in which a suitable vein is located by both visual and tactile inspection. Once an optimal insertion site is chosen, the clinician then guides the needle tip to the center of the target vessel, relying on visual and tactical feedback to assure a successful venipuncture. However, DVA can cause simple procedures to become challenging, time-consuming endeavors. Patients with DVA have either nonvisible, nonpalpable, or rolling/deforming vessels that create challenges in both identifying a suitable vessel and performing the needle stick. In these cases, failure rates are reported at 27% for patients without visible veins, 40% for patients without palpable veins, and 60% for patients who were emaciated[3,4]. Repeated failures to start an IV line have also been shown to significantly increase the likelihood of phlebitis, thrombosis, and blood transmission infections, and may necessitate obtaining central venous or arterial access, at much greater cost and risk[5–9]. As a result, venipuncture is one of the leading causes of injury to both patients[10,11] and clinicians[12–15]. Additionally, difficulties in obtaining venous access significantly lengthen the procedure time, ranging from 5 minutes to one hour, while also requiring additional personnel to complete[16]. In total, difficult venipuncture affects not only patients and clinicians but also the healthcare system as a whole, with costs estimated to exceed $4 billion per year in the United States alone[17–20].

Challenges associated with venipuncture have pushed for the development of technologies to assist clinicians in finding and identifying suitable vessels for insertion. Imaging technologies that use near-infrared (NIR) light can help visualize peripheral veins in the arm[8]. However, the penetration depth of NIR imaging is limited to ~3 mm in tissue, thus proving to be unsuitable for obese patients[21,22]. Moreover, research findings are unclear regarding the efficacy of NIR imaging systems to assist in venipuncture procedures[23–25]. Ultrasound imaging is the current standard of practice for assisting clinicians in obtaining

venous access in patients with DVA[26]. However, manual needle insertion under ultrasound guidance is challenging for less experienced personnel because of hand-eye coordination required for steady placement and control of both the probe and needle[16,27]. Overall, several studies investigating NIR and ultrasound imaging technology to assist in performing venipunctures observe no significant difference in success rates when compared with manual procedures, indicating that the actual insertion of the needle may prove to be the limiting factor in failed venipunctures, not the identification of a suitable vessel[23,28–30].

To address the challenges of DVA, our laboratory is developing an automated venipuncture device for obtaining venous access safely and reliably. Previously, we developed a benchtop venipuncture device for point-of-care blood analysis that featured a 9-degree-of-freedom (DOF) robotic system that utilized NIR imaging and computer vision processing to identify suitable vessels for cannulation and ultrasound imaging to guide the robotic needle insertion[22,31,32]. However, its large size, lack of mobility, and large number of DOF make it difficult to implement in a number of clinical scenarios requiring rapid venous access, especially in emergency situations where patient mobility is restricted. Additionally, we demonstrated this device's high success rates in phantom arms containing synthetic vessels; however, no human study has been performed to evaluate a robotic venipuncture device for in-human use.

In this paper, we present a miniaturized device for hand-held use and evaluate its blood drawing capabilities on human participants. The hand-held device combines high precision robotics with 2D ultrasound imaging to automatically guide an attached needle into the vessel center. The device is composed of three main components: (1) a 2-DOF robotic needle manipulator containing an electromagnetic needle loader and needle tip force sensor; (2) a 2D short-axis view ultrasound probe; and (3) a host processor. Further device operation can be found in the materials and methods section: robotic venipuncture device operation.

Here, we evaluate the safety, efficacy, and accuracy of the device in robotically placing a needle tip into a participant's median cubital vessel to draw a 5 mL sample of blood. We also hypothesize and discuss reasons for missed sticks in DVA groups and analyze ultrasound and force data retrieved from the procedures to guide future design enhancements. Lastly, we investigate the possibility of identifying failed venipunctures mid-insertion by utilizing ultrasound and force data retrieved during each procedure in order to improve future success rates.

HUMAN STUDY RESULTS

Hand-held venipuncture device and operation

In this study, a hand-held venipuncture device (Fig. 1a,b) was developed to robotically guide a 25G hypodermic needle into a peripheral forearm vessel for blood sampling. The hand-held device features a 2-DOF manipulator that both aligns the needle trajectory with the imaged vessel and inserts the needle with high precision and accuracy (Fig. 1b). An electromagnet, incorporated into the device, is used to hold and dispense of needles between the procedures. A force sensor is placed in-line with the needle axis to record forces during insertion. The device uses a 2D linear, short-axis orientation, ultrasound probe to image and

identify suitable vessels for cannulation. A custom ultrasound hydrogel clip is used to provide a dry acoustic interface between the ultrasound transducer head and skin (Fig. 1b). Further details of the attachable ultrasound gel clip and needle clip can be found in section "Materials and Methods".

Device operation during this human study was as follows. Once a suitable vessel was identified by the attending physician, the device was manually positioned over the chosen venipuncture site for ultrasound imaging (Fig. 1c–d). The device was positioned over the arm such that the ultrasound probe was perpendicular with the imaged vessel, as seen in Fig. 1c(**i**). The vessel coordinates, retrieved from the ultrasound images, were then used by the device to compute the necessary kinematics for needle insertion such that the needle tip reached the lumen center at the intersection of the ultrasound imaging plane (Fig. 1c(**ii-iii**)). After successful insertion, the needle tip can be seen in the center of the vessel lumen (Fig. 1e). A yellow dashed ellipse highlights the vessel wall in the ultrasound image, where the red and blue lines represent the vessel ellipse major and minor axes, respectively (Fig. 1e). Once successfully inserted, 5 mL of blood was drawn into a collection tube, after which the needle was retracted and dispensed. Detailed operational steps and further procedure protocol can be found in the methods section. A preview video of a blood draw procedure performed by the device can be seen in Supplementary Video 1[a].

Overall results

A total of 31 healthy adults participated in this study. Figure 2 shows the overall venipuncture success rates, and Table 1 shows the participant demographics and related data during each procedure. The participants were categorized into two groups: those who had DVA and those who did not (non-DVA)[4,16]. The criteria for DVA included having either >30 BMI or no visible veins identified. The basis for this definition of DVA is referenced in literature by Sebbane, Witting *et al.*[4,16]. Of the 31 participants in this study, six were considered to have DVA. The device demonstrated an overall success rate of 87% ($n = 31$) and a 97% success rate for the non-DVA group ($n = 25$). A venipuncture was considered successful if there was blood flow into the collection tube within two needle insertion attempts. The average procedure time for each blood draw was 93 ± 30 s ($n = 31$), with no difference in time between the DVA and non-DVA groups. A comparison of previous studies investigating venipuncture success rates showed that clinicians obtain an average of ~90% success rate on patients who are non-DVA and ~60% on patients who are considered to have DVA[3,4,16,33–35]. Given this, our results are consistent with success rates and procedure times typically observed for routine blood draws in non-DVA patients. No bruising, back vessel wall puncture, or inadvertent injuries occurred during the course of the study. Furthermore, the participants did not note or exhibit any excessive uncomfortableness or pain with the device or during the course of the blood draw.

[a]Supplementary Video 1 ("Venipuncture device performing blood draw procedure on a human participant") can be viewed at http://www.worldscientific.com/doi/suppl/10.1142/S2339547819500067

Device needle tip placement accuracy

Of the 31 participants in the study, the device failed to draw blood in four cases, three of which were DVA. Failure was likely attributed to the needle tip failing to puncture the initial vessel wall, either due to the vessel deforming or rolling out of the target position as the needle attempted to puncture the vessel. In these failed cases, while vessel displacement was large because of the needle insertion, the device still demonstrated high needle tip placement accuracy. Across all participants, the device achieved a robotic needle tip placement accuracy of 0.23 ± 0.17 mm, with respect to its target position (Fig. 3a). For comparison, the average target vessel size, given as ellipse major and minor axes (Fig. 3a, yellow dashed line) were 5.8 ± 1.4 mm and 3.8 ± 1.3 mm, respectively. However, while the needle tip placement error was low, four venipunctures still resulted in a missed stick during this study. By observing the needle tip position and vessel center post-puncture in unsuccessful cases, we see noticeable displacement in vessel position as a result of the needle insertion (Fig. 3b). Compared to successful cases, failed venipunctures (Fig. 3c, red box) displayed a larger degree of vessel displacement during needle insertions, with distances between needle tip and vessel center averaging 1.3 ± 0.5 mm ($n = 4$). Alternatively, successful venipuncture cases (Fig. 3c, blue box) showed lower displacements between the vessel center and final needle tip position, with values of 0.5 ± 0.3 mm ($n = 27$). Overall, these results indicate that while the device is accurate at placing the needle tip at its desired target, large vessel displacements, caused from the insertion itself, resulted in four of the 31 venipunctures to fail.

OPTIMIZING FUTURE VENIPUNCTURES

During each venipuncture procedure, the device collected pertinent ultrasound vessel imaging data, motor position encoder data, and force feedback data along the needle tip axis. In the next sections, we will investigate the relationships between the ultrasound and force feedback data with successful and unsuccessful venipunctures with the goal of improving future device performance and success rates for patients with DVA. By relating these data with previous venipuncture attempts, it may be possible for the device to predict the likelihoods of a failed venipuncture even before the needle tip has punctured the vessel wall. Learning from previous venipunctures, the device could make the necessary needle insertion adjustments in real time to assure the cannula is properly inserted into the target vessel.

Vessel displacements and cannulation success rates

Ultrasound imaging data of the target vessel were recorded during each venipuncture, illustrating the vessel displacement as the needle attempted to puncture and reach the vessel center. Identifying and quantifying these vessel displacements during the venipuncture may assist the device by compensating for displacements mid-insertion. Figure 4a shows a comparison between ultrasound images of a successful venipuncture on a non-DVA participant versus a DVA participant with a rolling vessel. Y-axis displacement represents the degree of vessel rolling, while Z-axis displacement is indicative of the vessel being pushed downward as the needle begins to puncture the vessel wall. In the successful case (Fig. 4a, top left and right image), little vessel movement is seen in both Y and Z axis directions. By examining the unsuccessful case (Fig. 4a, bottom left and right), a large

displacement to the right is seen as the vessel rolls out of the needle insertion path. When averaging for all 31 participants in this study (Fig. 4b), we see unsuccessful venipunctures exhibit a much higher *Y*-axis displacement (1.3 ± 0.15 mm) than their successful counterparts (0.3 ± 0.2 mm). A slightly larger *Z*-axis displacement average (Fig. 4c) is also seen in unsuccessful cases (0.3 ± 0.2 mm) than that observed in the successful ones (0.2 ± 0.2 mm). However, no statistical difference was found between these two groups ($p = 0.54$). Figure 4d highlights the degree of vessel rolling between the groups even further, showing the difference in vessel center coordinates before and after the vessel puncture. These results (Fig. 4d) highlight large vessel displacements occurring as a result of the needle pushing against the vessel. Observing this phenomenon mid-insertion, Fig. 4e shows the degree of vessel rolling as the needle makes its way toward its final target, the vessel center, as indicated by dashed line 2. Notably, however, in the unsuccessful cases, the vessel begins to roll out of the needle insertion path even before the needle tip has reached the vessel wall as indicated by the increase in *Y*-axis displacement just before dashed line 1 (Fig. 4e). This early vessel displacement may allow the device to detect a rolling vessel state before the puncture has occurred.

Needle insertion forces during venipunctures

Measuring forces along the needle axis mid-insertion may also provide a useful indicator of a successful vessel puncture. Clinicians note that during needle sticks, they can hapticly feel the puncturing of the vein wall[36]. For each participant, forces along the needle axis were recorded during each venipuncture. We then compared the force profiles of successful and unsuccessful cannulations at each needle insertion point (Fig. 5). These force profiles were averaged for all successful and unsuccessful cases, and were centered around the moment the needle tip encounters the vessel wall, known as the moment of puncture (dashed line 1). Successful cases demonstrated a higher average puncture force than the failed cases, with an average of 1.0 ± 0.5 N ($n = 27$) and 0.6 ± 0.3 N ($n = 4$), respectively (Fig. 5a,b). In the successful case (Fig. 5a, blue line), the force profile had a sharp peak at the moment of puncture (dashed line 1), followed by a drop in force as the needle continued toward the vessel center, and finally followed by a period of resting force at ~0.4 N when insertion stopped (dashed line 2). Conversely, the unsuccessful cases (Fig. 5a, red line) lacked a defined peak in force, but instead gradually increased in value until the needle insertion halted (dashed line 2). This observation is consistent with the ultrasound images at the time of puncture. In the unsuccessful cases, the needle tip does not puncture the vessel, but instead, continues its insertion path as the vessel either rolls out of position or collapses. Figure 5b confirms this assessment, showing a significant difference ($p = 0.048$) in puncture force between successful and unsuccessful cases.

Predicting failed venipunctures mid-insertion

Early detection of unsuccessful punctures could allow the device to adjust its insertion trajectory mid-insertion (for instance by adapting to vessel rolling and deformation), stop the insertion, or alert the physician. Our previous observations (Figs. 4e and 5b) suggest the importance of information contained in both the ultrasound image sequence and the measurements of force before and at the time of puncture. Specifically, we observed that slight vessel rolling can be seen occurring just before the moment of puncture, and forces in

successful cases also appear to peak in amplitude once the needle has punctured the vessel. To differentiate between successful and failed cannulations, and to predict such failures at an early moment in time, we applied a linear discriminant analysis (LDA) classification model utilizing the lateral (Y) displacement of the vessel (as determined from ultrasound) and the force measurements as predictors of failure (Fig. 6a). We evaluated the classification accuracy of the models along 0.1 mm increments during robotic needle insertion, thus capturing the change in predictive accuracy as a function of time. For example, at 0.5 mm prior to vessel puncture (Fig. 6a), the classification accuracy of the two-variable model is 100%, as the model has correctly plotted a boundary line separating successful and unsuccessful cases. We then compared the results to those of univariate predictions based on vessel Y-displacement or force alone (Fig. 6b). Further details of this model can be found in the methods section below, along with a video of the model running at each insertion increment (Supplementary Video 2[b]). Using just the Y-displacement and force profiles independently as predictors, the model shows a prediction accuracy of 86% at the very moment of vessel puncture. With force and Y-displacement combined, the LDA model correctly identified all successful and unsuccessful cases with 100% accuracy before the needle tip had punctured the vessel wall (Fig. 6b). Interestingly, the two-variable model achieved the same 86% accuracy as well, but ~1.0 mm earlier than the single-variable models did.

DISCUSSION

In this paper, we demonstrated the first-in-human use of a hand-held, ultrasound-guided, robotic venipuncture device for routine blood draws on healthy adult volunteers. The device demonstrated an overall success rate of 87% ($n = 31$) and a 97% success rate on non-DVA participants ($n = 25$), with a needle placement accuracy of 0.23 ± 0.17 mm and an average procedure time of 93 ± 30 s between all groups. Compared to clinical averages for manual venipuncture, the performance of our device was consistent with non-DVA cases (~90% success rate) and met or exceeded success rates and procedure times in DVA cases (~60% success rate)[3,4,34,35]. The device also performed comparable to venipunctures conducted under ultrasound guidance, with success rates reported in these studies at ~85%[33,37]. However, these studies did not specify the number of needle insertion attempts for a successful venipuncture. Compared to standard clinical procedure times, Witting *et al.* reported the incidence and median delays associated with IV access among 107 patients as 61%/1 min, 11%/5 min, 23%/15 min, and 5%/120 min[16]. Considering this, our device demonstrated a faster and more consistent procedure time across all participants, regardless of the presence of DVA factors. It should be noted that this study was not intended to show a direct comparison or benefit between the hand-held device and manual venipuncture. The intention of this device is to improve venipuncture success rates among all patient demographics, without requiring clinicians to have extensive past experience in obtaining venous access. Future work will involve follow-up studies on larger patient populations and a direct comparison between manual venipuncture, with and without ultrasound guidance, in terms of success rate and time to completion.

[b]Supplementary Video 2 (“Linear discriminate analysis model for predicting successful or unsuccessful venipunctures”) can be viewed at http://www.worldscientific.com/doi/suppl/10.1142/S2339547819500067

Previous iterations of the venipuncture device have been designed in our laboratory for benchtop use and were not manually operated by the user, as they were in this study. The motivation for the benchtop design was for performing high-throughput blood draw procedures that would be used in junction with a point-of-care blood diagnostic system, as is described by Balter *et al.*[32]. In this benchtop design, the device used NIR passive stereo imaging to identify a suitable insertion site on the patient's upper forearm area. Once found, the attached ultrasound probe was robotically lowered over the chosen site and the needle insertion commenced[22,31,32]. In the hand-held version demonstrated in this paper, ultrasound imaging is used alone for image guidance, as NIR imaging is no longer required because the user is now manually placing the device over the insertion site. Additionally, because NIR imaging is limited to penetration depths of ~3 mm in skin, it is unsuitable for identifying vessels in obese or high BMI patients who have vessels deeper than what can be detected with NIR[22]. This modification from benchtop to hand-held allows for greater portability and accessibility to patients who would otherwise not be able to access such a device, at the cost of requiring the user to manually place the device over the insertion area. However, we believe that the use of manual operation, compared to a completely automated benchtop, would bring comfort to patients who would otherwise be uneasy with having a robotic device performing blood draws without clinical supervision.

CONCLUSION AND FUTURE WORK

In this paper, we presented a hand-held venipuncture device capable of drawing blood from a peripheral forearm vein of human participants by using a combination of miniaturized robotics and ultrasound imaging. To improve clinical translation of the device, a number of enhancements could be made. Before the device can perform the needle insertion, the needle trajectory must be manually aligned and centered with the underlying vessel. This can become time-consuming, prone to trial and error, and require the device to be fixed and steadied once it is aligned and centered with the vessel. To improve this, we intend to add a third DOF to the device that will auto-align the needle trajectory path with the underlying vessel. This ensures that the needle is constantly centered with the ultrasound imaged vessel even during jittered movement caused from the user or patient. Furthermore, this would obviate the need for the operator to manually align the device, and instead require the user to simply place the device over the general area of insertion (i.e., upper forearm). Additionally, the needle is currently fixed at a 25° angle during insertion, assuming the ultrasound probe is perpendicular with the vessel. Increasing the angle of insertion may be more advantageous for high vessel rolling environments. Future work will include adding a motorized angle adjustment DOF to the device to vary the insertion angle during the venipuncture.

We demonstrated that an LDA model can be used to correctly predict successful and unsuccessful venipunctures just before the moment of puncture. By determining the probability that the needle will miss the vessel, the device could then make quick adjustments to its insertion parameters, such as angle of insertion and speed, in order to maximize the likelihood of a successful venipuncture. For example, if the vessel begins rolling preemptively, the device could adjust the angle of insertion, increase insertion speed, and adjust needle alignment to compensate for this rolling. However, further studies investigating the relationship between DVA characteristics, such as vessel rolling, and

certain insertion parameters will be required to develop a system that could optimize the needle insertion procedure. Sophisticated phantom arm models that mimic these DVA properties synthetically in patients could be used as a basis for training data in future machine learning algorithms for the device[38]. In the future, we will investigate combining predictive machine learning models, such as LDA, with the device kinematics in order to make rapid needle position corrections that would maximize the likelihood of a successful venipuncture, especially in DVA cases.

While this human study focused on routine blood draws, it should be noted that a device such as this can also be extended to other areas of vascular access. These areas include IV, peripheral and deep IV catheter placement, arterial line placement, and endovascular procedures. The combination of robotic needle placement and ultrasound guidance provides a framework for future applications in medical robotics.

MATERIALS AND METHODS

Recruitment and eligibility

This study was granted approval by the Rutgers Institutional Review Board. A total of 33 healthy volunteers were recruited for this study. A sample size of n = ~30 was chosen so that the sampling distribution would approach a normal distribution. Written informed consent was obtained from each participant before beginning of the study and possible consequences of this study were explained. Participation in this human study was strictly voluntary, and no preferences or exclusions were made outside the defined criteria for eligibility. Exclusion and inclusion criteria are listed in Supplementary Table 1. Two participants of the 33 recruited ones were excluded from continuing with the procedure due to having vessel depths deeper than the allowable 8 mm limit permitted by the use of 25G × ¾’ non-spring Vaculet blood collection needle. The participants were categorized into two groups: DVA and non-DVA. The criteria for DVA included having either: >30 BMI and/or no visible veins. The basis for these criteria is referenced by Sebbane, Witting *et al.*[4,16]. Data collection was stopped and the procedure was aborted in the event the patient exhibited unease, pain, or had requested the procedure to stop. No participants or operators were inadvertently injured during this study as a result of the device or needle stick.

Blood draw procedure steps

The steps for acquiring a 5 mL blood sample using the device were as follows. First, the attending clinician prepared the participant for blood draw by swabbing the upper forearm with an alcohol wipe. A tourniquet was then applied to the mid bicep to increase blood flow to suitable vessels. Once prepared, the participant placed their arm into the arm rest holder provided while the attending physician visually and tactilely identified a suitable vein for venipuncture. Once the arm was in place, the venipuncture device was initiated and the clock for measuring procedure time was started. The device was then lowered and placed over the selected insertion site. If no insertion site could be found by the physician, the ultrasound imaging probe was manually scanned across the upper forearm area until a suitable vessel for insertion was visually identified from the image stream. Once found, the device was manually aligned with the underlying vessel and was fixed in place using a Flexbar passive

arm device that was secured to the benchtop via suction adhesion. Once fixed, the vessel center in the ultrasound image was selected by the clinician and the device then proceeded with the blood draw. Device operational steps can be found below. Once the needle reached the intended target, a small amount of blood (5 mL) was drawn into a Becton Dickinson Vacutainer tube. If no blood flow was seen, the needle was retracted and the device was removed from the participant's arm and a new insertion site was chosen by the clinician, and the process was restarted. A venipuncture was considered successful if blood flow was seen from the needle into the blood collection tube within two insertion attempts. Once procedure was completed, the assisting clinician applied gauze and bandaged the insertion site area while the needle clip was dispensed of via electromagnetic drop into a biohazard sharps container.

Robotic venipuncture device operation

Once the participant was prepped for blood draw and the arm was placed into the arm rest, the device was initiated. Device initiation involved calibrating and zeroing the force sensor for data acquisition, inserting the needle clip into the device, and homing both the injection and *Z*-axis motors to their starting positions. A 25G × ¾' nonspring Vaculet blood collection needle was loaded into our custom needle clip to secure needle placement with the device. The needle clip was placed into the device and securely held via the device's electromagnet needle holder. The needle trajectory path was manually aligned and centered with the underlying vessel chosen by the attending physician. This was done via ultrasound by positioning the device on the participants forearm and moving the device manually until the vessel was within the acceptable boundaries of the needle trajectory path. Once the vessel was centered with the needle trajectory path (red line—Supplementary Fig. 1), the vessel center coordinates were manually chosen by the clinician from the display monitor. These coordinates were then used by the device to determine the necessary kinematics to ensure that the needle tip intersected the ultrasound imaging plane at the vessel center. Once aligned and steady, the operator then commenced with the insertion procedure, and the injection-axis (Inj-axis) DOF drove the attached needle tip forward until it reached its target position, the vessel center. Safety features were implemented into the software to prevent needle insertion overshoot, along with emergency controls for immediate procedure abortion in the event of injury or inadvertent circumstances. The angle of insertion was fixed at a 25° angle relative to the participant's forearm. A Honeywell FSG 0-5N force sensor, in-line with the needle-axis, recorded forces along the needle axis during insertion. A Telemed 2D linear ultrasound imaging probe, with a lateral field of view of 28 mm, was used for vessel imaging at depths between 0 and 30 mms. A customized, attachable, and disposable needle clip and ultrasound gel clip was used during each procedure. A detailed view of the device can be seen in Fig. 7.

Attachable needle clip and ultrasound gel clip

The device presented here also featured two consumable items used during each procedure: the ultrasound gel clip and the needle clip. We designed and 3D-printed an attachable ultrasound gel clip that provides a dry, acoustic coupling between the participants skin and ultrasound transducer. Liquid acoustic gels, which are typically used during ultrasound imaging, were not suitable for this procedure, as the insertion site must be clean and free of residue to ensure that the needle is not contaminated before puncturing the skin. The

hydrogel clip provided a dry interface, free of residue, while still allowing for quality ultrasound images to be retrieved without the use of liquid gels being applied to the patient's skin. An Aquaflex ultrasound gel pad, an aqueous, flexible and disposable hydrogel, was used as our hydrogel when creating our clips. Secondly, we have designed and developed a 3D-printed needle clip that secures the needle of choice to the device during venipuncture. We developed this needle clip attachment so that it can be applicable with a wide variety of needles and needle brands for various venipuncture procedures and insertion depths. Additionally, because an electromagnet is used for needle loading and dispensing between procedures, the device removes the need for clinicians to come into contact with the needle, thus limiting the number of accidental needle sticks that are still prevalent in today's healthcare workplace[13,15,18].

Linear discriminate analysis model

Input variables for the LDA model included the Y-displacement profiles (Fig. 4e), known as the degree of vessel rolling, and the forces along the needle tip during each procedure (Fig. 5b). The output of this prediction model was the predicted labeled class, either being successful or unsuccessful. This model was run at each needle insertion point between 0 and 21 mm, in increments of 0.1 mm. A video of this model can be seen in Supplementary Video 2. The model for linear discriminate analysis is given as follows:

$$\hat{y} = \arg \min_{y = 1, \ldots K} \sum_{k = 1}^{K} \hat{P}(k \mid x) C(y \mid k)$$

where $\hat{y}$ is the predicted classification, K is the number of classes $\hat{P}(k \mid x)$ is the posterior probability of class k for observation x, and $C(y|k)$ is the cost of classifying an observation as y when its true class is k. In this model, each class Y generates data X using a multivariate normal distribution. This model used the same covariance matrix for each class and only varied the mean. Supplementary Video 2 shows the LDA model in action at each insertion point, between 0 and 21 mm. The LDA model attempts to separate the successful and unsuccessful cases based on their inputted observations, or variables, by plotting a line between points. The equation for this line is as follows:

$$K + [x_1 \; x_2] \; L = 0$$

where K and L are the coefficients for the linear boundary between the classes. Unsuccessful cases in this model were weighted by a value of 5 due to low sample size for unsuccessful cases ($n = 4$). LDA was modeled andperformed using Matlabs Statistics and Machine Learning Toolbox[39].

Statistical analysis

A nonparametric, unpaired, two-sided *t*-test was used to determine significance when comparing the mean values between data sets, specifically the Matt-Whitney *t*-test. Data presented in this paper was expressed as mean ± SD. Results were considered significant

with $p < 0.05$. All results presented in the paper were significant, except for Fig. 4c, Z-axis displacement comparison between successful and unsuccessful cases.

Supplementary Material

Refer to Web version on PubMed Central for supplementary material.

ACKNOWLEDGMENTS

We thank the Rutgers University Biomedical Engineering Department and the Medical Device Development Center for providing support and resources to complete this study. We also thank Rene Schloss for her editorial assistance and Anil Shrirao for his assistance during the study.

Funding: This study was funded through the National Institute Health (NIH) R01 grant (R01EB020036) and the NIH-funded Rutgers biotechnology Training Program (T32GM008339).

REFERENCES

1. Alexandrou E et al. International prevalence of the use of peripheral intravenous catheters. J. Hosp. Med 10, 530–533 (2015). [PubMed: 26041384]
2. Center for Health Statistics, N. National Hospital Ambulatory Medical Care Survey: 2016 Emergency Department Summary Tables.
3. Carr PJ et al. Insertion of peripheral intravenous cannulae in the emergency department: Factors associated with first-time insertion success. J. Vasc. Access 17, 182–190 (2015). [PubMed: 26660037]
4. Sebbane M et al. Predicting peripheral venous access difficulty in the emergency department using body mass index and a clinical evaluation of venous accessibility. J. Emerg. Med 44, 299–305 (2013). [PubMed: 22981661]
5. Miliani K et al. Peripheral venous catheter-related adverse events: Evaluation from a multicentre epidemiological study in France (the CATHEVAL Project). PLoS One 12, e0168637 (2017). [PubMed: 28045921]
6. Lefrant J-Y et al. Risk factors of failure and immediate complication of subclavian vein catheterization in critically ill patients. Intensive Care Med. 28, 1036–1041 (2002). [PubMed: 12185422]
7. Sou V et al. A clinical pathway for the management of difficult venous access. BMC Nurs. 16, (2017).
8. Katsogridakis YL, Seshadri R, Sullivan C & Waltzman ML Veinlite transillumination in the pediatric emergency department. Pediatr. Emerg. Care 24, 83–88 (2008). [PubMed: 18277843]
9. Wallis MC et al. Risk Factors for peripheral intravenous catheter failure: A multivariate analysis of data from a randomized controlled trial. Infect. Control Hosp. Epidemiol 35(1), 63–68 (2014). doi:10.1086/674398 [PubMed: 24334800]
10. Walsh G Difficult peripheral venous access: Recognizing and managing the patient at risk. J. Assoc. Vasc. Access 13, 198–203 (2008).
11. Kuensting LL et al. Difficult venous access in children: Taking control. J. Emerg. Nurs 35, 419–424 (2009). [PubMed: 19748021]
12. Wilburn SQ & Eijkemans G Preventing needlestick injuries among healthcare workers: A WHO-ICN collaboration. Int. J. Occup. Environ. Health 10, 451–456 (2004). [PubMed: 15702761]
13. Singh S, Goel V, Kumar D & Lingaiah R Occurrence of needlestick and injuries among health-care workers of a tertiary care teaching hospital in North India. J. Lab. Physicians 9, 20 (2017). [PubMed: 28042212]
14. Zaidi M, Beshyah S & Griffith R Needle stick injuries: An overview of the size of the problem, prevention & management. Ibnosina J. Med. Biomed. Sci 2, 53 (2010).
15. Motaarefi H. Factors associated with needlestick injuries in health care occupations: A systematic review. J. Clin. Diagnostic Res 10(8), IE01–IE04 (2016). doi:10.7860/jcdr/2016/17973.8221

16. Witting MD IV access difficulty: Incidence and delays in an urban emergency department. J. Emerg. Med 42, 483–487 (2012). [PubMed: 22137793]
17. McCann M, Einarsdóttir H, Van Waeleghem J-P, Murphy F & Sedgewick J Vascular access management 1: An overview. J. Ren. Care 34, 77–84 (2008). [PubMed: 18498572]
18. Cooke CE & Stephens JM Clinical, economic, and humanistic burden of needlestick injuries in healthcare workers. Med. Devices Evid. Res 10, 225–235 (2017).
19. Armenteros-Yeguas V et al. Prevalence of difficult venous access and associated risk factors in highly complex hospitalised patients. J. Clin. Nurs 26, 4267–4275 (2017). [PubMed: 28165645]
20. Mannocci A et al. How much do needlestick injuries cost? A systematic review of the economic evaluations of needlestick and sharps injuries among healthcare personnel. Infect. Control Hosp. Epidemiol 37, 635–646 (2016). [PubMed: 27022671]
21. Bashkatov AN, Genina EA, Kochubey VI & Tuchin VV Optical properties of human skin, subcutaneous and mucous tissues in the wavelength range from 400 to 2000 nm. J. Phys. D. Appl. Phys 38, 2543–2555 (2005).
22. Chen A, Nikitczuk K, Nikitczuk J, Maguire T & Yarmush M Portable robot for autonomous venipuncture using 3D near infrared image guidance. Technology 1, 72–87 (2013). [PubMed: 26120592]
23. de Graaff JC et al. Near-infrared light to aid peripheral intravenous cannulation in children: A cluster randomised clinical trial of three devices. Anaesthesia 68, 835–845 (2013). [PubMed: 23763614]
24. Fukuroku K, Narita Y, Taneda Y, Kobayashi S & Gayle AA Does infrared visualization improve selection of venipuncture sites for indwelling needle at the forearm in second-year nursing students? Nurse Educ. Pract (2016). doi:10.1016/j.nepr.2016.02.005
25. Peterson KA, Phillips AL, Truemper E & Agrawal S Does the use of an assistive device by nurses impact peripheral intravenous catheter insertion success in children? J. Pediatr. Nurs 27(2), 134–143 (2012). doi:10.1016/j.pedn.2010.10.009 [PubMed: 22341192]
26. Maecken T & Grau T Ultrasound imaging in vascular access. Crit. Care Med 35, S178–S185 (2007). [PubMed: 17446777]
27. Saranteas T Limitations in ultrasound imaging techniques in anesthesia: Obesity and muscle atrophy? Anesth. Analg 109, 993–994 (2009). [PubMed: 19690282]
28. Juric S, Flis V, Debevc M, Holzinger A & Zalik B Towards a low-cost mobile subcutaneous vein detection solution using near-infrared spectroscopy. Sci. World J 2014, 1–15 (2014).
29. Curtis SJ et al. Ultrasound or near-infrared vascular imaging to guide peripheral intravenous catheterization in children: A pragmatic randomized controlled trial. Can. Med. Assoc. J 187, 563–570 (2015). [PubMed: 25897047]
30. Bair AE, Rose JS, Vance CW, Andrada-Brown E & Kuppermann N Ultrasound-assisted peripheral venous access in young children: A randomized controlled trial and pilot feasibility study. West. J. Emerg. Med 219, (2008).
31. Balter ML, Chen AI, Maguire TJ & Yarmush ML Adaptive kinematic control of a robotic venipuncture device based on stereo vision, ultrasound, and force guidance. IEEE Trans. Ind. Electron 64, 1626–1635 (2017). [PubMed: 28111492]
32. Balter ML et al. Automated end-to-end blood testing at the point-of-care: Integration of robotic phlebotomy with downstream sample processing. Technology 6, 59–66 (2018). [PubMed: 30057935]
33. Brannam L, Blaivas M, Lyon M & Flake M Emergency nurses utilization of ultrasound guidance for placement of peripheral intravenous lines in difficult-access patients. Acad Emerg Med 11, 1361–1363 (2004). [PubMed: 15576530]
34. Chinnock B, Thornton S & Hendey GW Predictors of success in nurse-performed ultrasound-guided cannulation. J. Emerg. Med 33, 401–405 (2007). [PubMed: 17976752]
35. Lininger RA Pediatric peripheral i.v. insertion success rates. Pediatr. Nurs 29(5), 351–354. [PubMed: 14651305]
36. Dhingra N et al. WHO guidelines on drawing blood: Best practices in phlebotomy. World Heal. Organ 1–105 (2010). doi:10.1038/nature16040

37. Carter T, Conrad C, Link Wilson J & Dogbey G Clinical study ultrasound guided intravenous access by nursing versus resident staff in a community based teaching hospital: A (Noninferiority) trial. Emerg. Med. Int (2015). doi:10.1155/2015/563139

38. Chen AI et al. Multilayered tissue mimicking skin and vessel phantoms with tunable mechanical, optical, and acoustic properties. Med. Phys 43, 3117–3131 (2016). [PubMed: 27277058]

39. The MathWorks, I. MATLAB Statistics and Machine Learning Toolbox Release 2018b. (2019).

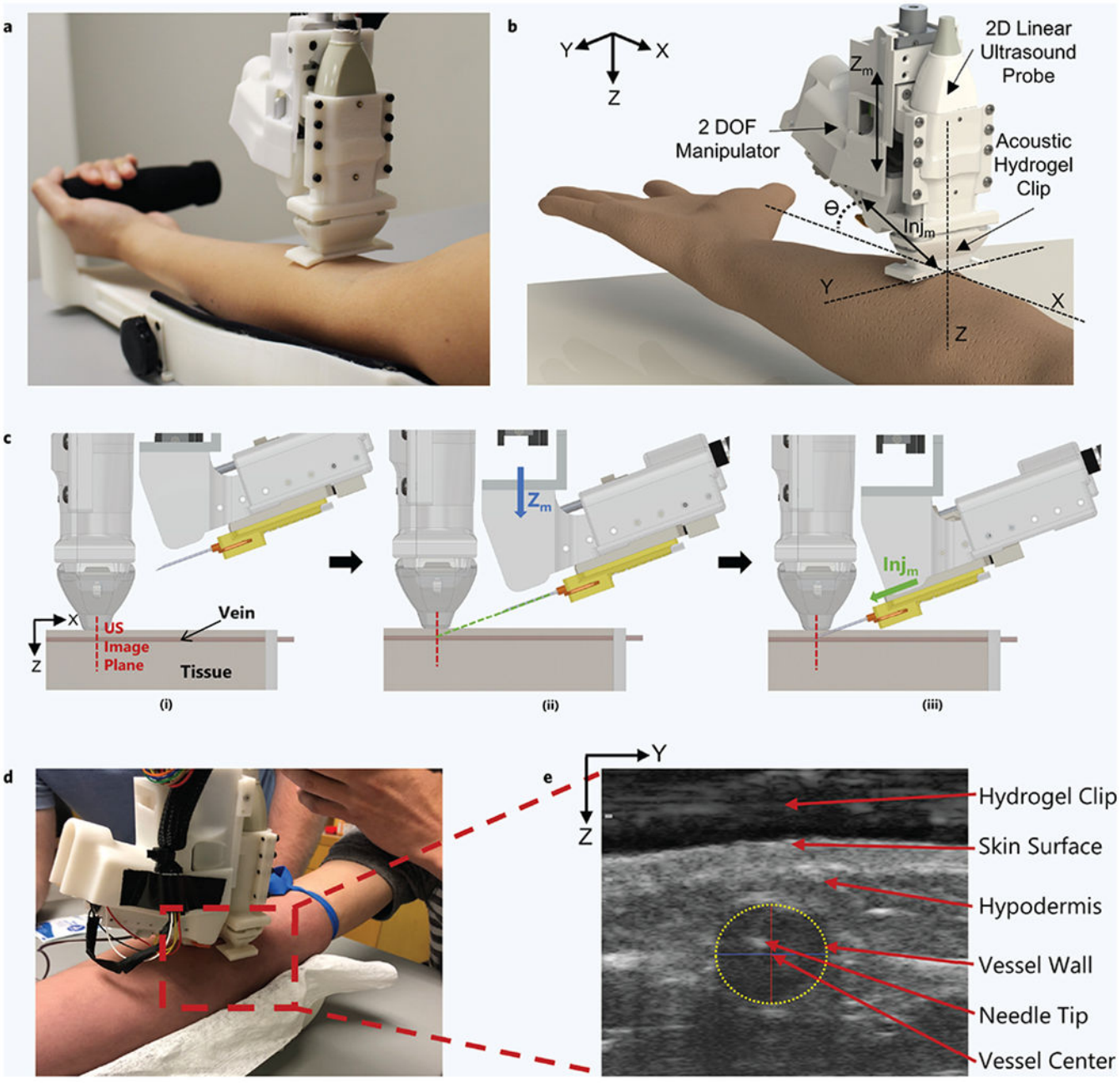

Figure 1. Robotic device set-up and operation.

(**a**) Hand-held venipuncture device. (**b**) Computer-aided design (CAD) displaying key components of the 2-degree-of-freedom (DOF) device. Angle of insertion (θ) is fixed at 25°. (**c**) Device operation. (i) Ultrasound (US) imaging plane provides a cross-sectional view of target vessel. (ii) Once a vessel is located by the device, the needle is aligned via the Z_m – DOF motor (Z_m = Z-axis motion). The Z_m motor (blue arrow) is responsible for aligning the needle trajectory with the vessel depth (Z-axis) to ensure the needle tip reaches the vessel center exactly at the ultrasound imaging plane. (iii) Once trajectory is aligned, the needle is inserted via the Inj_m – DOF (Inj_m = Injection motion) motor (green arrow) and automatically

halted once the tip has reached the vessel center. (**d**) Device positioned over the upper forearm during the study. (**e**) Ultrasound image depicting the needle tip present in the target vessel after a successful venipuncture. Vessel wall is identified by a yellow dashed ellipse. The *Z*-axis in the image indicates the vessel depth and the *Y*-axis indicates the sagittal position of the vessel. Positions of the vessel and needle tip are recorded with respect to the ultrasound transducer head (top of image).

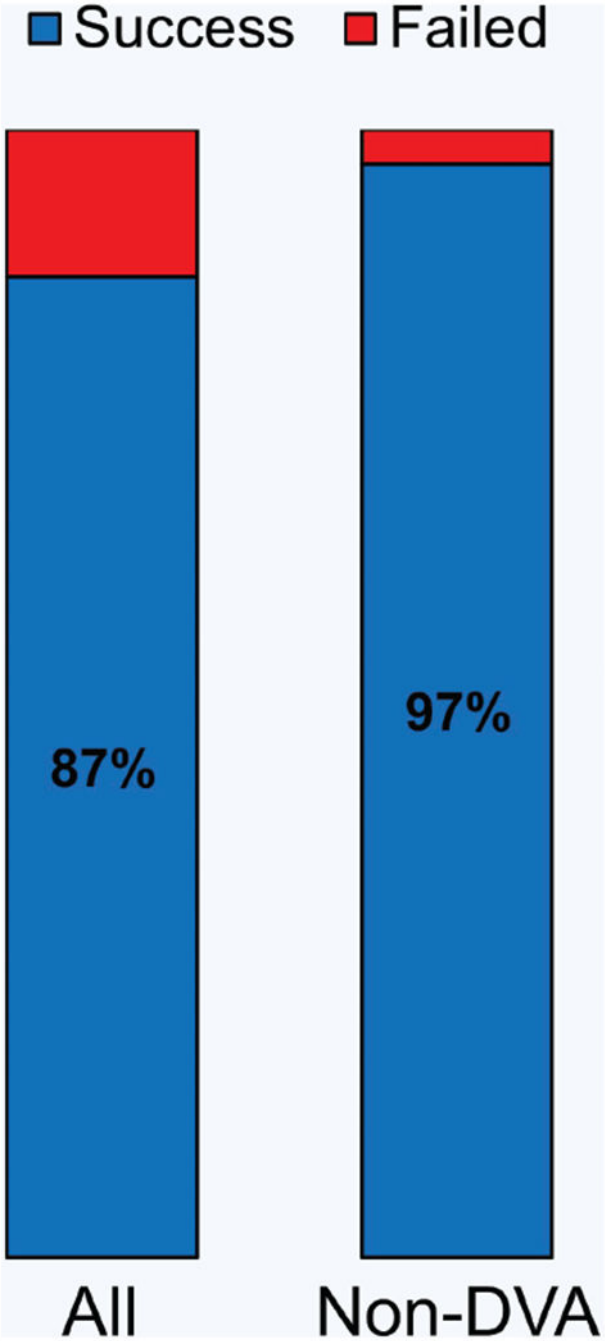

Figure 2. Venipuncture success rates.

Venipuncture success rate between all patients (n = 31) and non-difficult venous access (DVA) patients (n = 25). Average number of insertion attempts = 1.2.

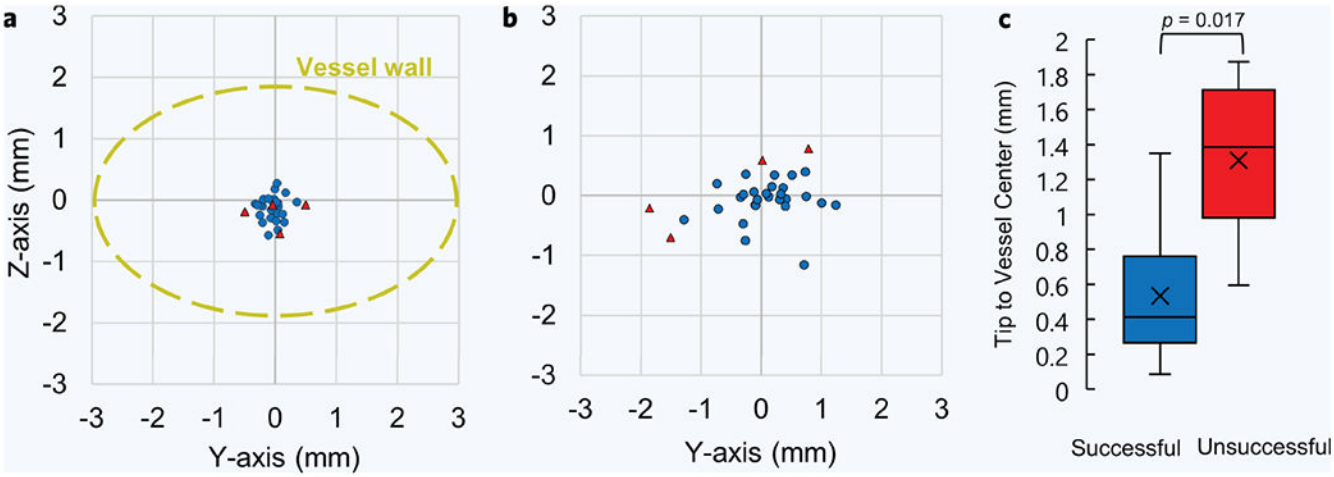

Figure 3. Needle tip placement accuracy and vessel sizes.

(**a**) Needle tip placement accuracy from all participants ($n = 31$). This is the difference between the desired and actual needle tip position after robotic insertion was completed, as determined from the ultrasound images. Blue points are the needle tip coordinates from successful cases and red are from unsuccessful cases. The *Z*-axis is the vessel depth and the *Y*-axis is the vessel sagittal position, as determined from the ultrasound images. Displayed in yellow is the average vessel size from all participants, which is shown for perspective. (**b**) Distances between the needle tip position and the vessel center, post-puncture. Needle tip and vessel center positions were obtained from ultrasound images, relative to the transducer head, during each venipuncture. (**c**) Distribution of differences between needle tip position and vessel center, post-puncture, between successful and unsuccessful venipunctures. *P* value was calculated using an unpaired nonparametric two-sided *t*-test.

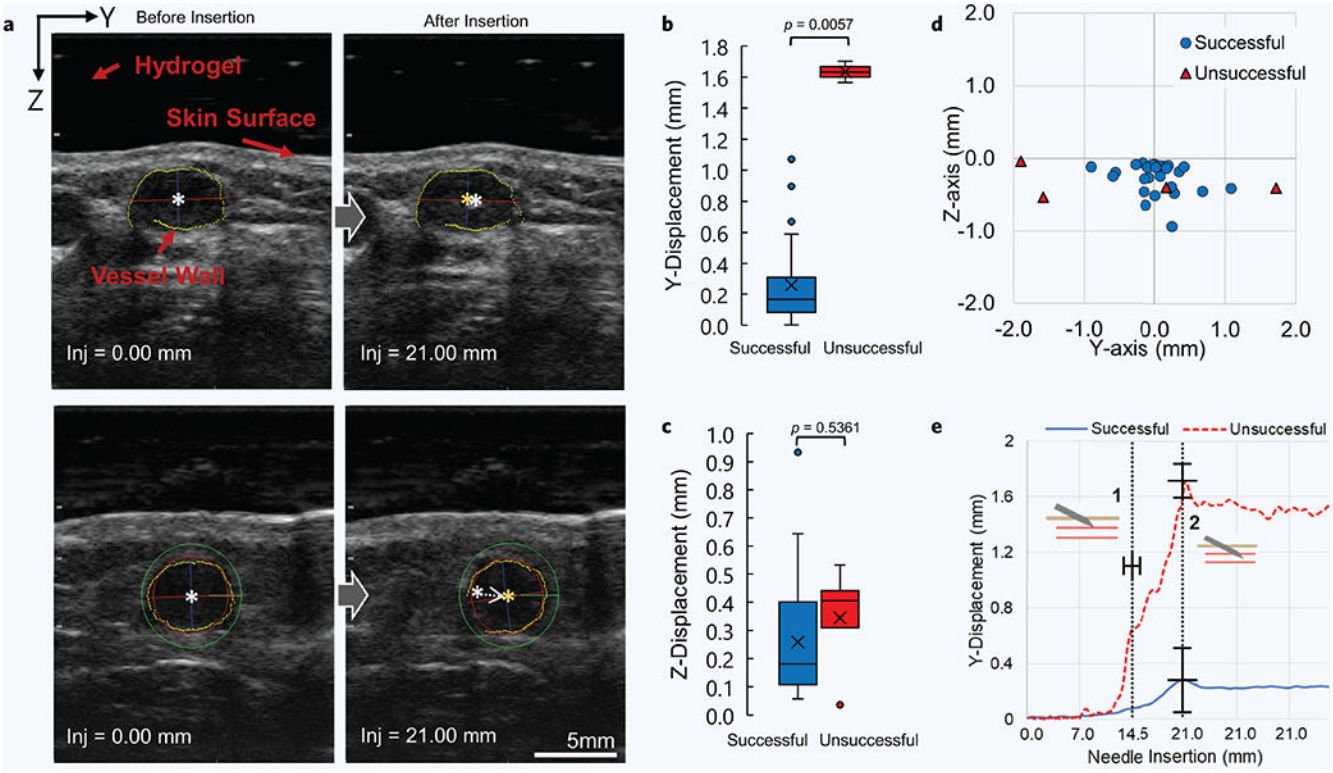

Figure 4. Vessel displacements during needle insertion.

(**a**) Ultrasound images of target vessel before (left images) and after (right images) the needle has reached its final target. Top images show successful venipuncture with minimal vessel displacement. Bottom images show unsuccessful venipuncture with noticeable vessel displacement. White star indicates vessel center before puncture. Orange star indicates vessel center after puncture. (**b-c**) *Y*-axis and *Z*-axis vessel displacement comparison between all successful ($n = 27$) and unsuccessful ($n = 4$) blood draws, respectively. *P* values were calculated using an unpaired nonparametric two-sided *t*-test. (**d**) Difference in vessel center position as a result of the needle puncturing the vessel. This is the difference between the orange and white star coordinates seen in "a" above, but for all 31 participants. (**e**) Combined average of *Y*-vessel displacements during each recorded needle insertion distance between all cases ($n = 31$). Data between both groups were centered around the moment the needle tip encounters the vessel wall, also known as the moment of puncture. The moment of puncture between all procedures occurred at 14.6 ± 1.2 mms. Dashed line 1 indicates the moment of puncture and dashed line 2 indicates the needle reaching its final target position and halting. Error bars represent mean ± SD.

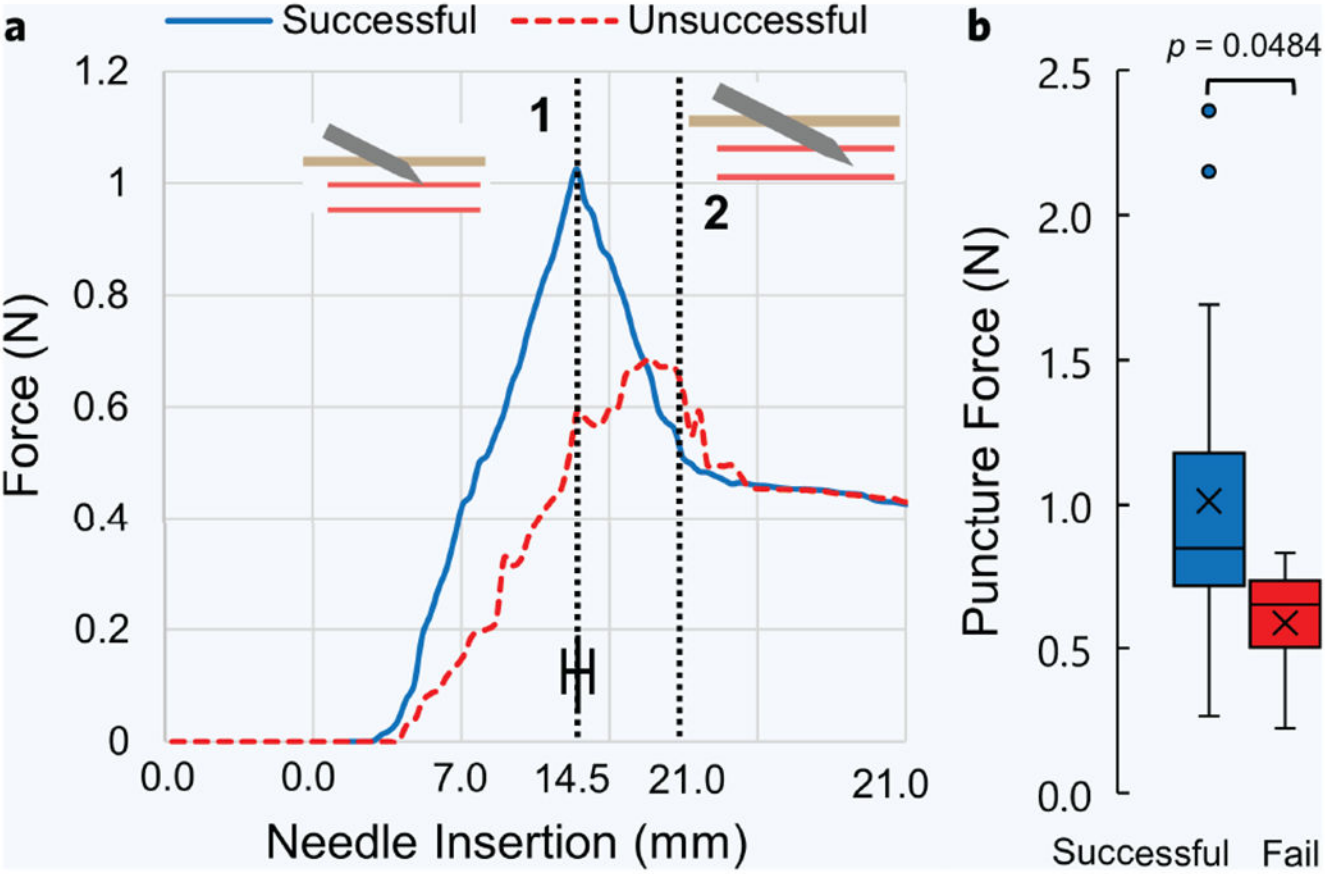

Figure 5. Puncture force between successful and unsuccessful venipunctures.

(**a**) Average force profiles between successful ($n = 27$) and unsuccessful ($n = 4$) venipunctures. Force profiles between all patients were centered and averaged around the moment of puncture, indicated by dashed line 1. Dashed line 2 represents the moment when the needle tip reached the vessel center and insertion halted. (**b**) Distribution of all forces at the moment of puncture between successful and unsuccessful cases. Error bar represents mean ± SD. *P* values were calculated using an unpaired nonparametric two-sided *t*-test.

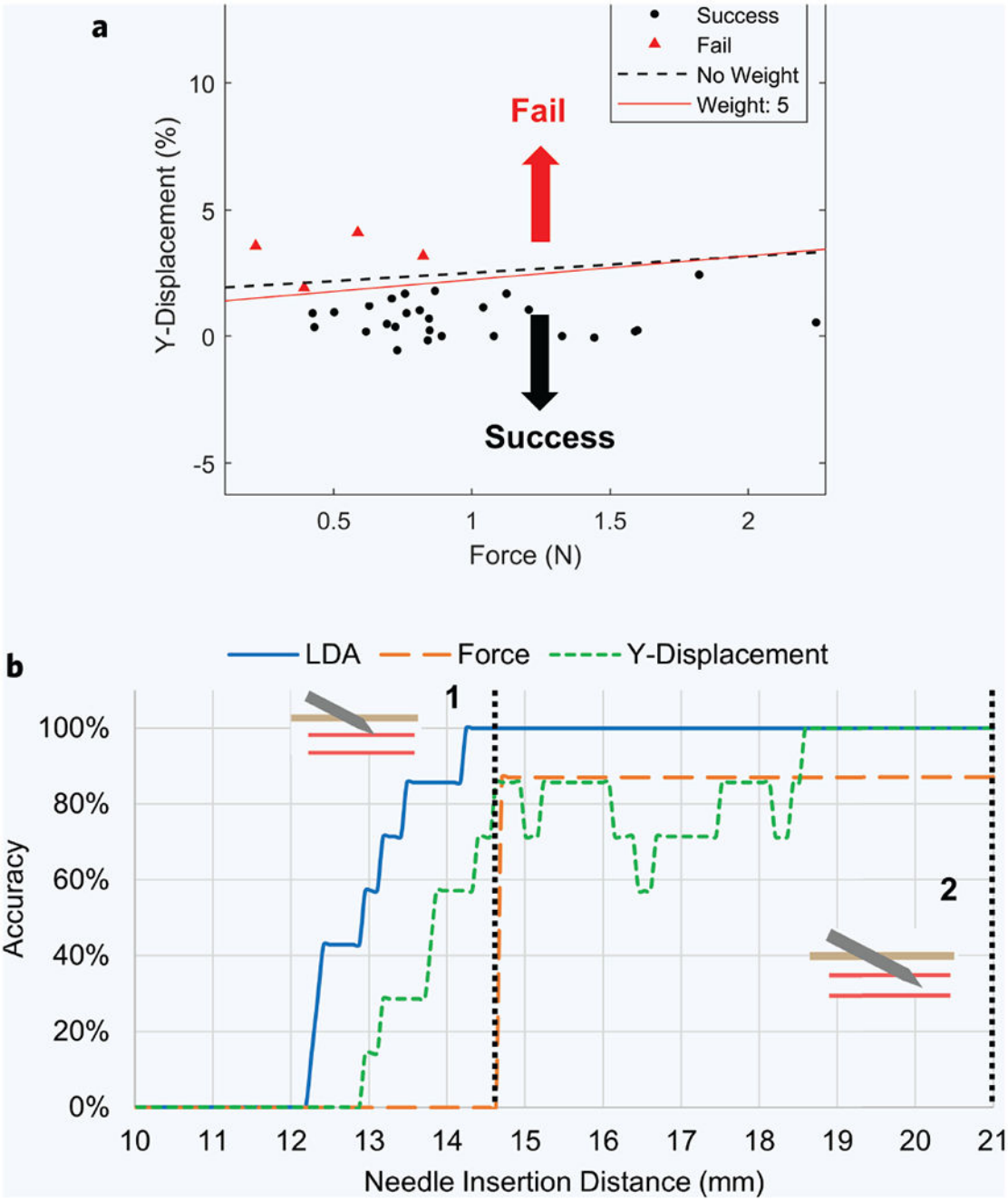

Figure 6. Predicating a successful puncture mid-insertion using the linear discriminate analysis (LDA) model.

(**a**) Visualization of the LDA model 0.5 mm prior to vessel puncture ($n = 31$). The red line is the weighted discrimination, and the dashed line is unweighted. Points above the line are labeled as failure and points below the line are labeled as successful by the predictor. (**b**) LDA model accuracy at each needle insertion recording point, between 0 and 21 mm. Accuracy is the percentage that the LDA model correctly identified whether each venipuncture was successful or unsuccessful. Dashed line 1 and 2 represent the moment of

vessel puncture and when the needle tip has reached the vessel center and insertion stopped, respectively.

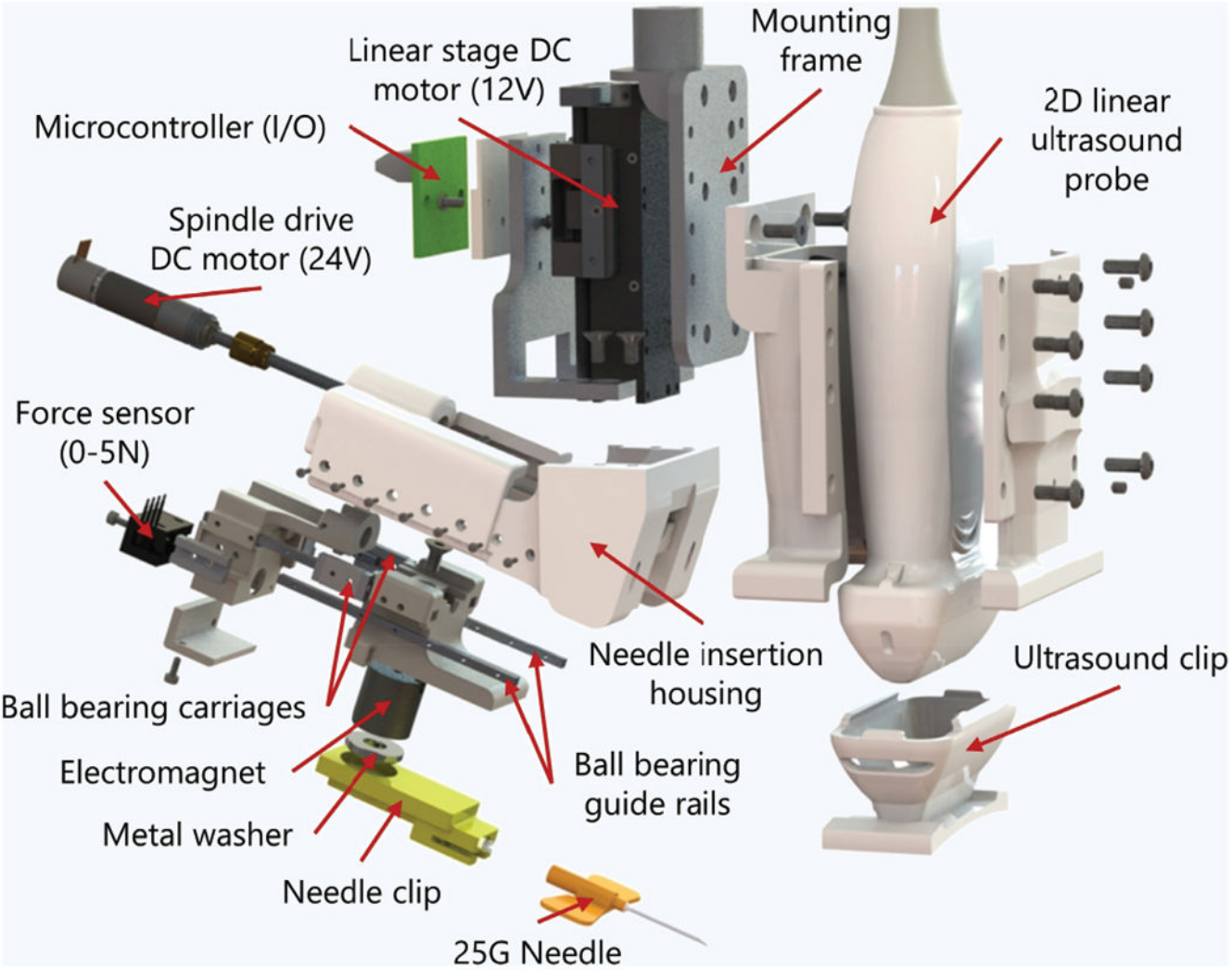

Figure 7.
Exploded view and component listing of the hand-held venipuncture device.

Table 1

Participant demographics and results.

Participant	Sex	Skin tone (Type)	BMI (kg/m^2)	Success	Time (s)	Vein visible
1	M	III	19.1	Y	115	Y
2	M	II	26.4	Y	121	Y
3	F	II	21.0	Y	110	Y
4	F	IV	26.4	Y	50	Y
5	F	IV	21.9	Y	78	Y
6	F	III	19.5	N	110	Y
7	M	V	24.4	Y	202	Y
8	F	V	19.9	Y	69	Y
9	M	II	29.8	Y	80	Y
10	M	II	31.2	N	52	Y
11	M	II	22.2	Y	62	Y
12	M	II	22.2	Y	76	Y
13	F	II	23.2	Y	62	Y
14	M	IV	37.8	N	125	N
15	F	III	22.3	Y	72	Y
16	M	II	25.8	Y	92	Y
17	F	III	19.7	Y	55	Y
18	M	I	19.6	Y	84	Y
19	M	II	39.7	Y	73	N
20	M	III	22.9	Y	125	Y
21	M	II	29.8	Y	132	Y
22	M	III	19.6	Y	65	Y
23	F	II	20.4	Y	80	N
24	F	III	30.2	N	121	N
25	M	II	19.7	Y	78	Y
26	M	III	25.9	Y	115	Y
27	F	III	21.6	Y	63	Y
28	F	I	26.6	Y	86	Y
29	M	II	23.7	Y	48	Y
30	F	II	23.1	Y	72	N
31	M	II	22.0	Y	135	Y